Original Article

Identification of a lactate metabolism-related lncRNAs signature for predicting the prognosis in patients with kidney renal clear cell carcinoma

Tianzi Xu[1,2#^], Yixin Liu[1,2#], Biao Ning[1,2], Min Luo[1,2], Yongchang Wei[1,2^]

[1]Department of Radiation and Medical Oncology, Zhongnan Hospital of Wuhan University, Wuhan University, Wuhan, China; [2]Hubei Key Laboratory of Tumor Biological Behaviors, Zhongnan Hospital of Wuhan University, Wuhan University, Wuhan, China

Contributions: (I) Conception and design: T Xu, Y Wei; (II) Administrative support: M Luo, Y Wei; (III) Provision of study materials or patients: M Luo, Y Wei; (IV) Collection and assembly of data: T Xu; (V) Data analysis and interpretation: Y Liu, B Ning, M Luo; (VI) Manuscript writing: All authors; (VII) Final approval of manuscript: All authors.

[#]These authors contributed equally to this work.

Correspondence to: Min Luo, MD, PhD; Yongchang Wei, MD, PhD. Department of Radiation and Medical Oncology, Zhongnan Hospital of Wuhan University, No. 169, Donghu Road, Wuchang District, Wuhan 430071, China; Hubei Key Laboratory of Tumor Biological Behaviors, Zhongnan Hospital of Wuhan University, Wuhan University, Wuhan, China. Email: 15172327560@163.com; weiyongchang@whu.edu.cn.

Background: Lactate metabolism-related (LMR) long noncoding RNAs (lncRNAs) play significant roles in various cancers, but their impact on kidney renal clear cell carcinoma (KIRC) remains unclear. This study aimed to explore the value of LMR lncRNA and develop a risk model for KIRC.

Methods: Data on KIRC patients were downloaded from The Cancer Genome Atlas (TCGA) database. LMR lncRNAs were identified by co-expression, univariate and multivariate analyses, and least absolute shrinkage selection operator (LASSO) regression analysis. Subsequently, a prognostic signature was constructed and its accuracy was verified. To predict the prognosis of KIRC effectively, we established a nomogram based on this information. Enrichment analysis, tumor mutational burden (TMB) analysis, immune status and the therapeutic sensitivities of KIRC patients were also investigated. Quantitative real-time polymerase chain reaction (qRT-PCR) was performed to detect the expression of lncRNAs.

Results: We constructed and verified a predictive signature based on six LMR lncRNA (*LINC00944*, *AC090772.3*, *Z83745.1*, *AP001267.3*, *AC092296.1*, and *AL162377.1*) to assess the patient prognoses of KIRC. Survival analyses showed a more unfavorable outcome in high-risk patients (P<0.001). Enrichment analysis demonstrated that immune-related pathways were enriched in the high-risk group. Besides, patients classified by risk scores had distinguishable immune status, TMB, response to immunotherapy, and sensitivity to chemotherapy and targeted drugs.

Conclusions: The LMR lncRNAs signature has significant implications for prognostic assessment and clinical treatment guidance in KIRC.

Keywords: Kidney renal clear cell carcinoma (KIRC); lactate metabolism; long noncoding RNA (lncRNA); gene signature; immune checkpoint

Submitted Sep 19, 2023. Accepted for publication Feb 18, 2024. Published online Apr 18, 2024.
doi: 10.21037/tau-23-483
View this article at: https://dx.doi.org/10.21037/tau-23-483

^ ORCID: Tianzi Xu, 0009-0000-3009-6398; Yongchang Wei, 0000-0001-7205-4663.

Introduction

Renal cell carcinoma (RCC) is the third most common primary malignancies in the urogenital system, accounting for approximately 2% of newly diagnosed malignancies (1,2). Of the various subtypes of RCC, kidney renal clear cell carcinoma (KIRC) is the most frequent and deadly subtype (3), characterized by high heterogeneity and metastatic potential (4). Surgery is the primary therapeutic approach for KIRC due to its bad sensitivity to chemotherapy and radiotherapy (5). Nevertheless, distant metastases that develop after surgery remain in a high proportion of patients (3). Despite therapeutic advances in immunotherapy and molecular targeted therapy (6,7), a significant proportion of patients do not respond to cancer treatment or even experience serious side effects (8,9). Consequently, it is imperative to explore potential prognostic markers for KIRC patients that may help to improve curative effect while reducing the burden of the disease.

Compelling evidence has suggested tumor cells select glycolysis as their primary energy source regardless of oxygen availability and that is known as the Warburg effect (10,11). Once perceived as a metabolic end product of glycolysis, lactate now also acts as an important modulator affecting the biological properties of surrounding cells (11,12). Notably, lactylation, which reflects the level of lactate, has a well-documented tight association with cancer hallmarks, including metabolic reprogramming, tumour-associated inflammation, and immunosurveillance evasion (11). It has been reported that tumor lactate levels are closely related to tumor progression, maintenance and treatment resistance (13,14). Targeting lactate metabolism in tumors has been considered as a potential antitumor therapeutic strategy (13,15). Currently, further work is needed to understand the role of lactate metabolism in KIRC and its impact on immune regulation, as well as its mechanisms of synergistic effect with current immunotherapies.

Long noncoding RNAs (lncRNAs) are non-protein-coding transcripts with nucleotide sequences longer than two hundred (16,17). The lncRNAs are involved in a wide range of biological processes, including modulating gene expression, various physiological and pathological processes (17-20). Flourishing evidence has warranted that their aberrant expressions are closely related to tumor malignancy (17,21), indicating that lncRNAs may be putative candidates for prognostic markers in malignant tumors. However, there has been little research on lncRNAs related to lactate metabolism, and their functions also remain unclear in KIRC.

Here, we established a lactate metabolism-related (LMR) lncRNAs prognostic signature, and appraised its clinical value through enrichment analysis, tumor mutational burden (TMB) analysis, drug sensitivity and differential analysis of tumor immune status in KIRC patients. The findings of this study have the potential to provide us with novel perspectives for improving existing diagnostic, therapeutic and prognostic predictions for KIRC patients. We present this article in accordance with the TRIPOD reporting checklist (available at https://tau.amegroups.com/article/view/10.21037/tau-23-483/rc).

Highlight box

Key findings

- We established and validated a predictive signature based on six lactate metabolism-related long noncoding RNAs (LMR lncRNAs) to provide a nuanced evaluation of patient prognoses in kidney renal clear cell carcinoma (KIRC) and thus developed a new predictive tool for clinical settings.

What is known and what is new?

- Flourishing evidence already warrants that cancer-related lncRNAs play an important role in promoting malignant phenotypes and may be putative candidates for prognostic markers in malignant tumors.
- We are the first to develop and validate a predictive signature of survival based on six LMR lncRNAs to provide insight into KIRC patient prognoses and elucidate their relationships with tumor immune status.

What is the implication, and what should change now?

- These findings not only deepen our comprehension of the interplay between LMR lncRNAs and KIRC but also hold far-reaching implications for advancing personalized therapeutic strategies and precision medicine in oncology.

Methods

Data source and preparation

The RNA sequencing (RNA-seq) transcriptome data (mRNA and lncRNA expression data) and clinicopathological data of KIRC samples were extracted from The Cancer Genome Atlas (TCGA) database (https://portal.gdc.cancer.gov/). We obtained 515 TCGA samples with complete survival data and complete RNA-seq data. Then we divided the 515 TCGA patients into training set

Table 1 Clinical information of the training set and test set

Characteristic	Entire set (n=515)	Validation cohort		
		Training set (n=259)	Test set (n=256)	P value
Age (years), median [IQR]	60 [51, 69]	61 [51, 70]	60 [52, 69]	0.83
Gender, n (%)				0.27
Female	177 (34.4)	95 (36.7)	82 (32.0)	
Male	338 (65.6)	164 (63.3)	174 (68.0)	
Grade, n (%)				0.77
G1	12 (2.3)	6 (2.3)	6 (2.3)	
G2	220 (42.7)	112 (43.2)	108 (42.2)	
G3	201 (39.0)	105 (40.5)	96 (37.5)	
G4	74 (14.4)	32 (12.4)	42 (16.4)	
Gx	8 (1.6)	4 (1.5)	4 (1.6)	
Stage, n (%)				0.68
Stage I	256 (49.7)	127 (49.0)	129 (50.4)	
Stage II	56 (10.9)	30 (11.6)	26 (10.2)	
Stage III	117 (22.7)	63 (24.3)	54 (21.1)	
Stage IV	83 (16.1)	37 (14.3)	46 (18.0)	
Unknown	3 (0.6)	2 (0.8)	1 (0.4)	
T stage, n (%)				0.97
T1	262 (50.9)	131 (50.6)	131 (51.2)	
T2	68 (13.2)	33 (12.7)	35 (13.7)	
T3	174 (33.8)	89 (34.4)	85 (33.2)	
T4	11 (2.1)	6 (2.3)	5 (2.0)	
N stage, n (%)				0.18
N0	230 (44.7)	126 (48.6)	104 (40.6)	
N1	16 (3.1)	7 (2.7)	9 (3.5)	
NX	269 (52.2)	126 (48.6)	143 (55.9)	
M stage, n (%)				0.53
M0	408 (79.2)	207 (79.9)	201 (78.5)	
M1	79 (15.3)	36 (13.9)	43 (16.8)	
Mx	28 (5.4)	16 (6.2)	12 (4.7)	

IQR, interquartile range.

(n=259) and test set (n=256) in a 1:1 ratio. *Table 1* shows the demographic characteristics of patients in the two cohorts. Progression-free survival (PFS) data were retrieved from the GDC hub of UCSC Xena browser (https://gdc.xenahubs.net). The study was conducted in accordance with the Declaration of Helsinki (as revised in 2013).

Identified LMR genes and lncRNAs

A total of 284 LMR genes were extracted from the

Molecular Signatures Database (https://www.gsea-msigdb.org/gsea/msigdb/index.jsp). Then we calculated the LMR lncRNAs expression profile in normal and tumor tissues, and identified differentially expressed lncRNAs [|log fold change (FC)| >1, false discovery rate (FDR) <0.05] via the "limma" R package. To screen differentially expressed LMR lncRNA, the Pearson correlation analysis (|Cor| >0.4, P<0.001) and differential analysis (|logFC| >1, FDR <0.05) were also used.

Development and verification of a LMR lncRNAs prognostic signature

In the training set, we initially utilized univariate Cox regression analysis to identify LMR lncRNAs associated with the prognosis of KIRC patients. Subsequently, we conducted least absolute shrinkage selection operator (LASSO) regression analysis and multivariate Cox regression analysis to determine the LMR lncRNAs necessary for establishing a prognostic signature. Cytoscape software and the ggalluvial R software package were adopted to visualize the LMR lncRNAs. The risk score was calculated using the format:

$$risk\ score = \sum_{i=1}^{n} coefficient(i) * lncRNA(i) expression \quad [1]$$

Data were classified into two risk groups based on median risk score. The Kaplan-Meier curve was utilized to explore the difference in survival rates between the two groups. The receiver operating characteristic (ROC) curves and the area under the curves (AUC) were applied to verify the accuracy of the signature. Finally, the signature was verified in the test set and the overall set. Principal component analysis (PCA) was performed for dimensionality reduction and quality control.

Construction of a prognostic nomogram

The prognostic value of the risk score and clinical features was verified by the univariate and multivariate Cox regression analyses. By integrating the risk score with clinical features, we established a prognostic nomogram for predicting overall survival (OS) of KIRC patients. Afterward, calibration curves were used to evaluate the reliability and accuracy of the nomogram.

Gene set enrichment analysis (GSEA) and immune infiltration analysis

We utilized the GSEA software (Version 4.2.3) to investigate the potential functions between the two risk groups, and the results were depicted with by enrichment maps. The single sample gene-set enrichment analysis (ssGSEA) was performed to quantify and compare the immune status in the low- and high-risk groups. Besides, the expression of immune checkpoints was also explored in the two risk groups.

Somatic mutation analysis and investigation of drugs sensitivity

The mutation landscapes of KIRC patients were also procured from the TCGA database. The "maftools" R package was used to analyze the somatic mutations in KIRC patients in the two risk groups. The half-maximal inhibitory concentration (IC50) of common drugs were calculated to evaluate the power of the signature in predicting the treatment response, using the "pRRophetic" R package. The Wilcoxon signed-rank test was applied to compare IC50 between high- and low-risk groups.

Cell culture

Human RCC cell lines 786-O, and ACHN, and normal kidney HK-2 cells were purchased from the Institute of Biochemistry and Cell Biology, Chinese Academy of Science (Shanghai, China), maintained in the suggested media, and incubated at 37 ℃ in a 5% CO_2 incubator.

RNA extraction and quantitative real-time polymerase chain reaction (qRT-PCR)

Total RNA was extracted with Trizol reagent (Vazyme, Cat# R401-01, Nanjing, China), and cDNA was obtained by reverse transcription process using Hifair II Strand cDNA Synthesis Super Mix (Cat# 11120ES60, Yeasen, Shanghai, China) based on the product instructions. Quantitative real-time polymerase chain reaction (qRT-PCR) was carried out with the CFX Connect Detector instrument (Bio-Rad, Hercules, CA, USA) and the relative mRNA expression level was calculated by the $2^{-\Delta\Delta Ct}$ method (22). The primer sequences of genes are presented in Table S1.

Statistical analysis

All statistical analyses were performed using R software (Version 4.2.2) and Perl programming language (Version 5.32.1). Wilcoxon rank-sum test was applied to compare

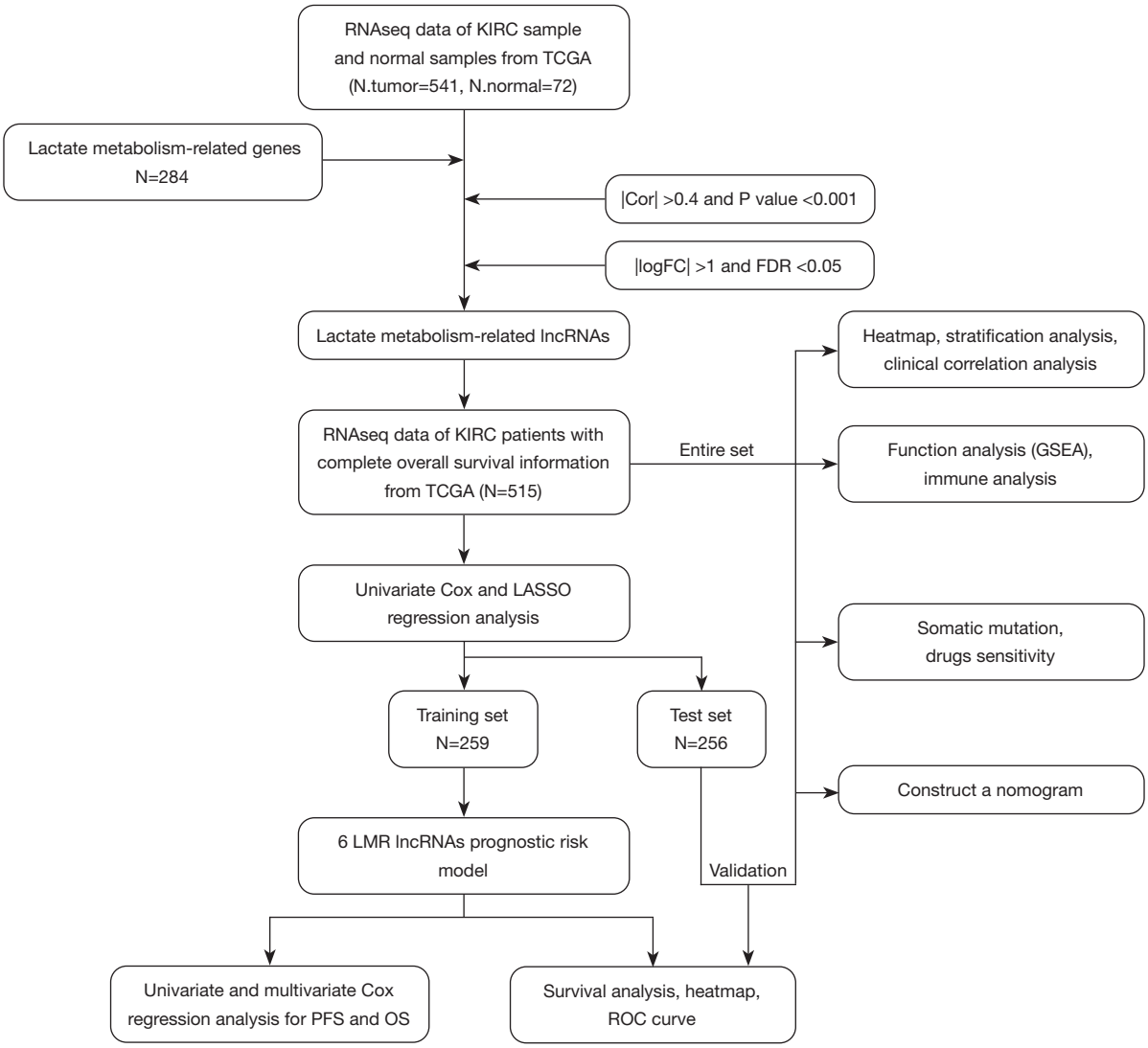

Figure 1 Research flow chart. KIRC, kidney renal clear cell carcinoma; TCGA, The Cancer Genome Atlas; FC, fold change; FDR, false discovery rate; lncRNAs, long noncoding RNAs; GSEA, gene set enrichment analysis; LASSO, least absolute shrinkage and selection operator; LMR, lactate metabolism-related; PFS, progression-free survival; OS, overall survival; ROC, time-dependent receiver operating characteristic.

different groups. Pearson analysis was used to analyze the correlation between continuous variables. A P value <0.05 indicated statistical significance, unless stated otherwise.

Results

Establishing of a LMR lncRNAs prognostic signature in training set

The flowchart of our research is presented in *Figure 1*. Volcano plot and heatmap plot were utilized to show the genes correlated with lactate metabolism that had differential expression (*Figure 2A*,*2B*). We employed Pearson correlation analysis (|Cor| >0.4 and P<0.001) to explore the LMR-lncRNAs. Subsequently, differential analysis (|logFC| >1, FDR <0.05) was performed to identify differential expression LMR-lncRNAs (*Figure 2C*). Ultimately, a total of 1,454 LMR-lncRNAs with significant differential expression were selected for subsequent bioinformatics analysis. To further filter survival-related lncRNAs, lasso regression analysis and Cox regression

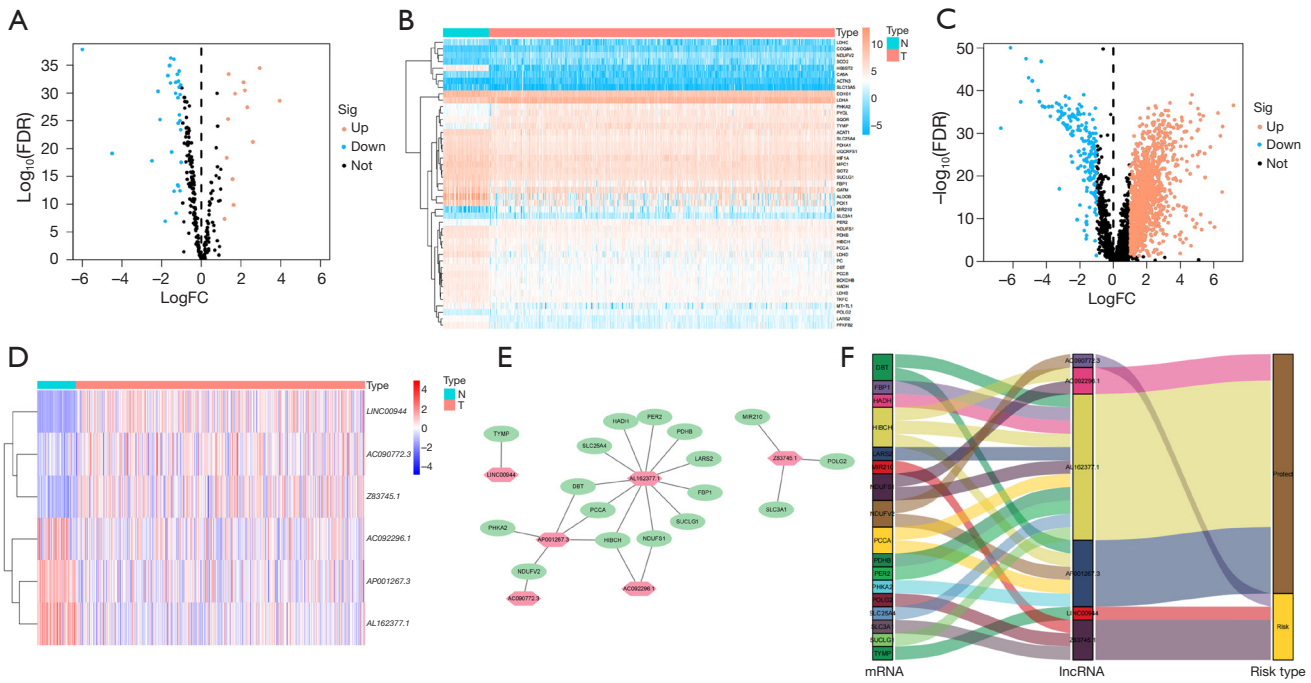

Figure 2 Screening for the lactate metabolism-related prognostic lncRNAs differentially expressed in the KIRC. (A,B) Volcano plot and heatmap of differentially expressed LMR genes. (C) Expression profile of the differentially expressed LMR lncRNAs. (D) Heatmap of the prognostic-related LMR lncRNAs. (E) Network of LMR-mRNAs and prognostic-related LMR lncRNAs. (F) Sankey diagram of prognostic-related LMR lncRNAs. lncRNAs, long noncoding RNAs; KIRC, kidney renal clear cell carcinoma; FDR, false discovery rate; FC, fold change; LMR, lactate metabolism-related; N, normal; T, tumor.

analysis were adopted to screen the candidate lncRNAs, and 6 LMR lncRNAs were finally identified. Among them, *LINC00944*, *AC090772.3* and *Z83745.1* were risk factors while *AP001267.3*, *AC092296.1* and *AL162377.1* were protective factors. *Figure 2D* shows the expression levels of the six LMR lncRNAs in KIRC patients. The network depicted the co-expression relationship of 23 pairs lncRNA-mRNA (*Figure 2E*). Sankey diagram further visualized the correspondence and regulation between the LMR lncRNAs and LMR mRNAs (*Figure 2F*). Multivariate Cox regression analysis was employed to build the LMR lncRNAs prognostic signature. The following equation was utilized to compute the risk score: risk score = (0.837418 × *LINC00944*) + (0.567824 × *AC090772.3*) + (0.346777 × *Z83745.1*) – (0.586784 × *AL162377.1*) – (0.803884 × *AC092296.1*) – (0.879993 × *AP001267.3*).

According to the median risk score, the KIRC patients were split to low- and high-risk subgroups. As demonstrated in *Figure 3A*, survival outcomes in the high-risk group were significantly worse than in the low-risk group. The 3- and 5-year survival rates were 63.9% and 49.3% for the high-risk group and 90.5% and 86.6% for the low-risk group, respectively. Moreover, the scatter plot also indicated that patients in the high-risk group tend to have shorter survival times than those in the low-risk group; the plot of the risk score distribution depicted that high-risk group had higher risk scores than low-risk group; the heatmap revealed differences in the expression profiles of six LMR lncRNAs between the low- and high-risk subgroups (*Figure 3B-3D*). In addition, ROC curves showed that the AUC values of survival outcomes were 0.783 in 1 year, 0.762 in 3 years, and 0.803 in 5 years (*Figure 3E*), respectively, indicating that the signature harbored a superior ability for prognosis prediction.

Validation of the LMR lncRNAs prognostic signature in test set and entire set

To verify the stability of the prognostic signature, the same algorithm and the same cut-off value were used to apply in the test set and entire set (*Figure 4*). Similarly, patients in the high-risk group possessed the worse survival outcomes

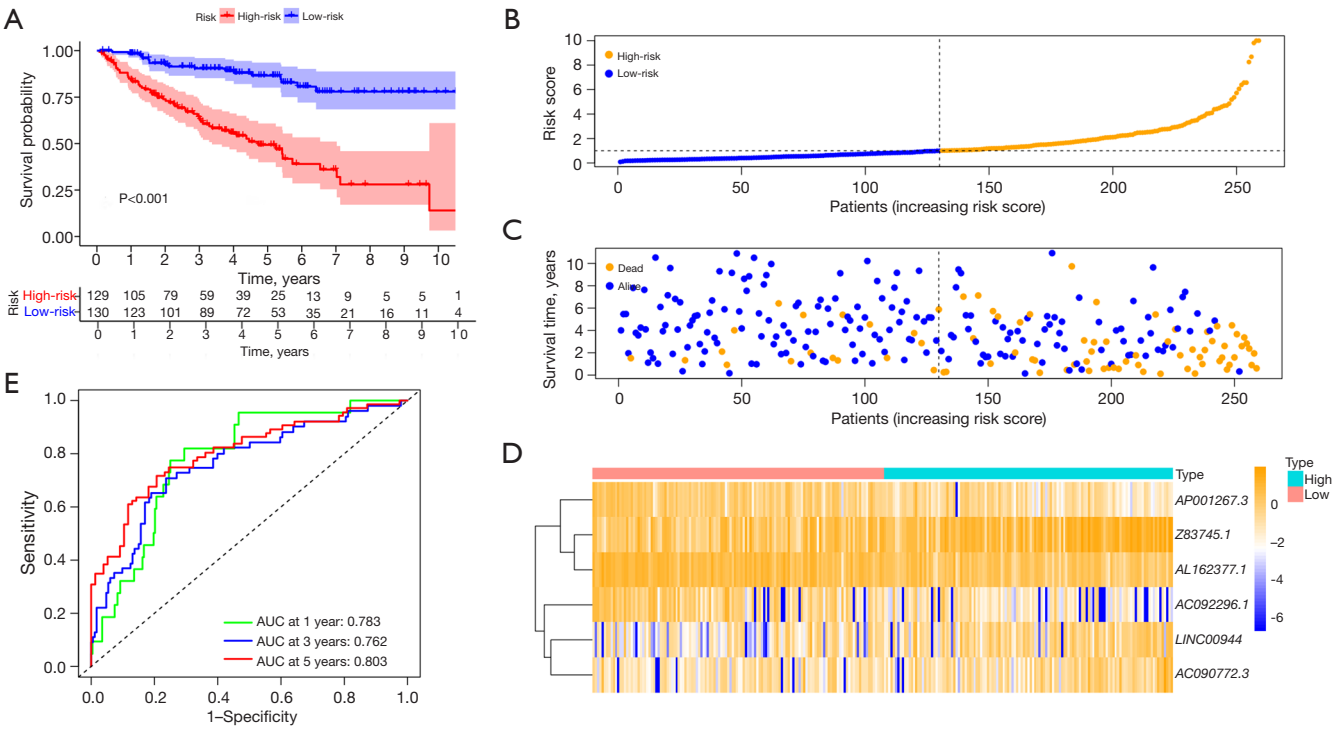

Figure 3 Results of prognostic analysis of risk score in training set. (A) Survival curves of the KIRC patients in different risk groups. (B) Rank of prognostic index and distribution of the two risk groups. (C) Survival status of patients in different groups. (D) Heatmap of expression profiles of prognostic-related LMR lncRNAs in two risk groups. (E) Time-dependent ROC curves of the risk score for the 1-, 3- and 5-years OS. KIRC, kidney renal clear cell carcinoma; LMR, lactate metabolism-related; lncRNAs, long noncoding RNAs; ROC, time-dependent receiver operating characteristic; AUC, area under the curve; OS, overall survival.

than those in the test set (*Figure 4A*) and the overall set (*Figure 4F*). Plots of the distribution of risk score, survival status, as well as the expression profiles of the six LMR lncRNAs were all shown to be in line with those in the training set (*Figure 4B-4D*,*4G-4I*). The AUC value corresponding to 1, 3, 5 years of survival outcomes were 0.802, 0.752, and 0.764 in the test set (*Figure 4E*), and 0.795, 0.759 and 0.783 in the entire set (*Figure 4J*), respectively. These results indicated that the LMR lncRNAs prognostic signature developed from the training set was highly accurate and robust.

Verification with qRT-PCR

To further validate the feasibility of the prognostic signature, we explored the expression levels of *LINC00944* and *AC092296.1* in normal kidney cells and two clear-cell RCC cell lines by qRT-PCR assays. The results showed that the expression level of *LINC00944* was significantly increased in renal cancer cells compared with normal kidney cells, whereas *AC092296.1* was downregulated in renal cancer cells (*Figure 5A*,*5B*). This finding further confirms the reliability of the signature.

Clinical correlation analysis

To evaluate the clinical significance and application of the prognostic signature, we integrated risk scores and other clinicopathological characteristics. As can be seen in *Figure 5C*, the heatmap illustrated the relationships between the clinicopathological characteristics of the two risk-subgroups and the expression profiles of the six LMR lncRNAs. Additionally, we discovered that there were substantial differences between the high- and low-risk groups in terms of tumor grade, American Joint Committee on Cancer (AJCC) stage, T, M, and survival status (*Figure 5D-5G*). To better access the clinical value and application of the prognostic signature, we carried out

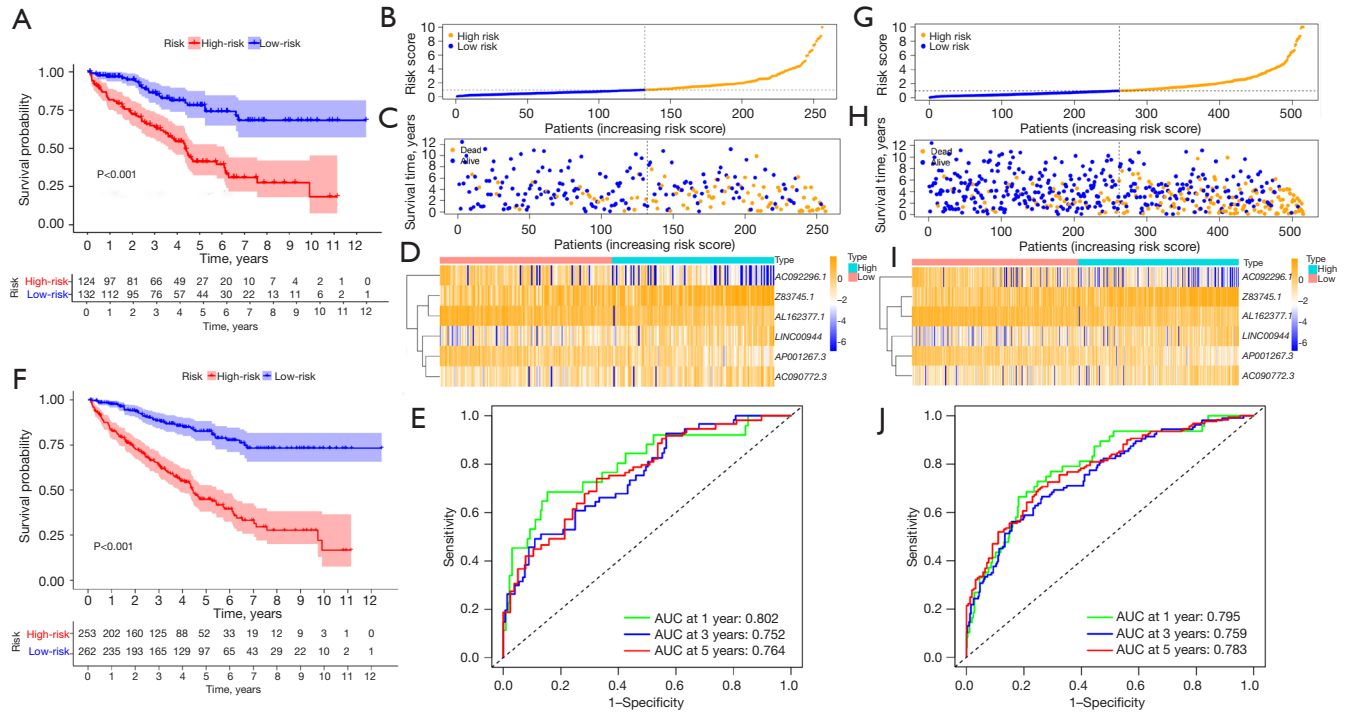

Figure 4 Results of prognostic analysis of risk score in validation sets. (A) Survival curve of KIRC patients in different risk groups in test set. (B) Rank of prognostic index and distribution of high and low-risk groups in test set. (C) Survival status of patients in different groups in test set. (D) Heatmap of expression profiles of prognostic-related LMR lncRNAs in two risk groups in test set. (E) Time-dependent ROC curves of the risk model for 1-, 3-, and 5-year OS in test set. (F) Survival curve of KIRC patients in different risk groups in entire set. (G) Rank of prognostic index and distribution of high and low-risk groups in entire set. (H) Survival status of patients in different groups in entire set. (I) Heatmap of expression profiles of prognostic-related LMR lncRNAs in two risk groups in entire set. (J) Time-dependent ROC curves of the risk model for 1-, 3-, and 5-year OS in entire set. KIRC, kidney renal clear cell carcinoma; LMR, lactate metabolism-related; lncRNAs, long noncoding RNAs; ROC, time-dependent receiver operating characteristic; AUC, area under the curve; OS, overall survival.

stratified analyses based on clinicopathological variables, including age, gender, grade, AJCC stages, T stage and M stage. For each different classification, patients in the high-risk group tended to have worse OS than that patients in the low-risk group (*Figure 6*).

Construction of a nomogram model

To identify parameters related to the prognosis of KIRC patients, univariate and multivariate regression Cox regression analyses were performed (*Figure 7A*,*7B*). Results confirmed that the risk score, age, stage, and M stage were independent prognostic predictors. Additionally, the multivariate ROC curve demonstrated that the signature outperformed other clinicopathologic parameters in terms of prognostic predictiveness (*Figure 7C*). The AUC value for the LMR lncRNAs signature was 0.775, which was greater than the AUC value for age (0.594), gender (0.485), grade (0.625), AJCC stage (0.688), T stage (0.664), M stage (0.634). Following that, we integrated the risk score with prognostic clinical indicators to construct a nomogram that can predict 1-, 3-, and 5-year survival rates of KIRC patients (*Figure 7D*). The calibration curves revealed an excellent match between predicted values and actual observations (*Figure 7E-7G*). Moreover, the concordance index value of the nomogram was 0.793, confirming its great accuracy.

Predictive value of the LMR lncRNAs signature for PFS

To further understand the underlying correlation of the risk score with the progression of KIRC, we performed survival analyses for PFS (*Figure 8A*). In the whole cohort, univariate Cox regression revealed that grade, stage, T and M stage were associated with the PFS of KIRC patients (*Figure 8B*).

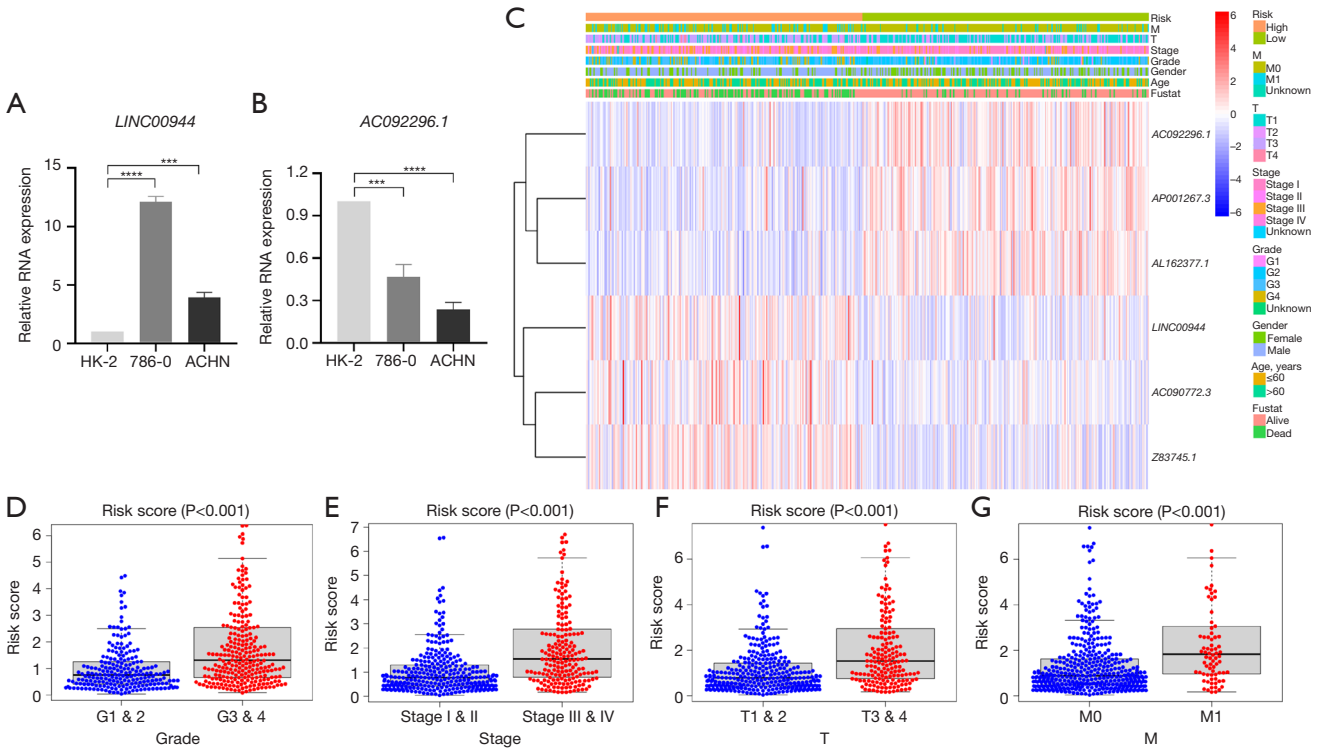

Figure 5 Expression levels and clinical value of the LMR lncRNAs. (A,B) The expression levels of *LINC00944* and *AC092296.1* in normal kidney cell and KIRC cells. (C) Distribution heatmap of the seven included lncRNAs and clinicopathological parameters in high- and low-risk groups. (D-G) Clinic relevance of the risk score, including tumor grade, AJCC stage, stage T, and stage M. ***, P<0.001; ****, P<0.0001. LMR, lactate metabolism-related; lncRNAs, long noncoding RNAs; KIRC, kidney renal clear cell carcinoma; AJCC, American Joint Committee on Cancer; M, metastasis; T, tumor.

Then, the multivariate Cox regression analysis (*Figure 8C*) was performed, and it confirmed that risk score [hazard ratio (HR), 1.126; 95% confidence interval (CI): 1.081–1.172; P<0.001] remained to be independent risk factor for PFS after controlling for other confounding factors. ROC curves (AUC: risk score =0.749, age =0.541, gender =0.554, grade =0.660, stage AUC =0.762, T =0.703 and M =0.683) showed that risk had a superior prediction value compared to most clinical information (*Figure 8D*). Overall, our results indicated that the LMR lncRNAs signature could serve as a good independent predictor of survival outcomes in patients with KIRC.

PCA and gene enrichment analysis

PCA was employed to assess the differences between the low-risk and high-risk groups based on all genes (*Figure 9A*), LMR genes (*Figure 9B*) and risk score-related genes (*Figure 9C*). The results of PCA displayed that the signature can effectively distinguish patients. To comprehend the biological processes in the low- and high-risk groups, we performed GSEA with the expression data of the samples. The results showed that the altered genes in the high-risk group were highly concentrated in immune-related biological processes, involving intestinal-immune-network-for-IgA-production, primary-immunodeficiency, autoimmune-thyroid-disease, allograft-rejection and asthma (*Figure 9D*), indicating possible role of the risk score in immunity. Besides, tight-junction, ErbB-signaling-pathway, glycerolipid-metabolism, adipocytokine-signaling-pathway and insulin-signaling-pathway were dominant in the low-risk group (*Figure 9E*). These outcomes revealed that the high-risk and low-risk groups had different immune- and metabolism-related genes, which might contribute to partially explain the significant prognosis difference. In addition, some other pathways were also differentially

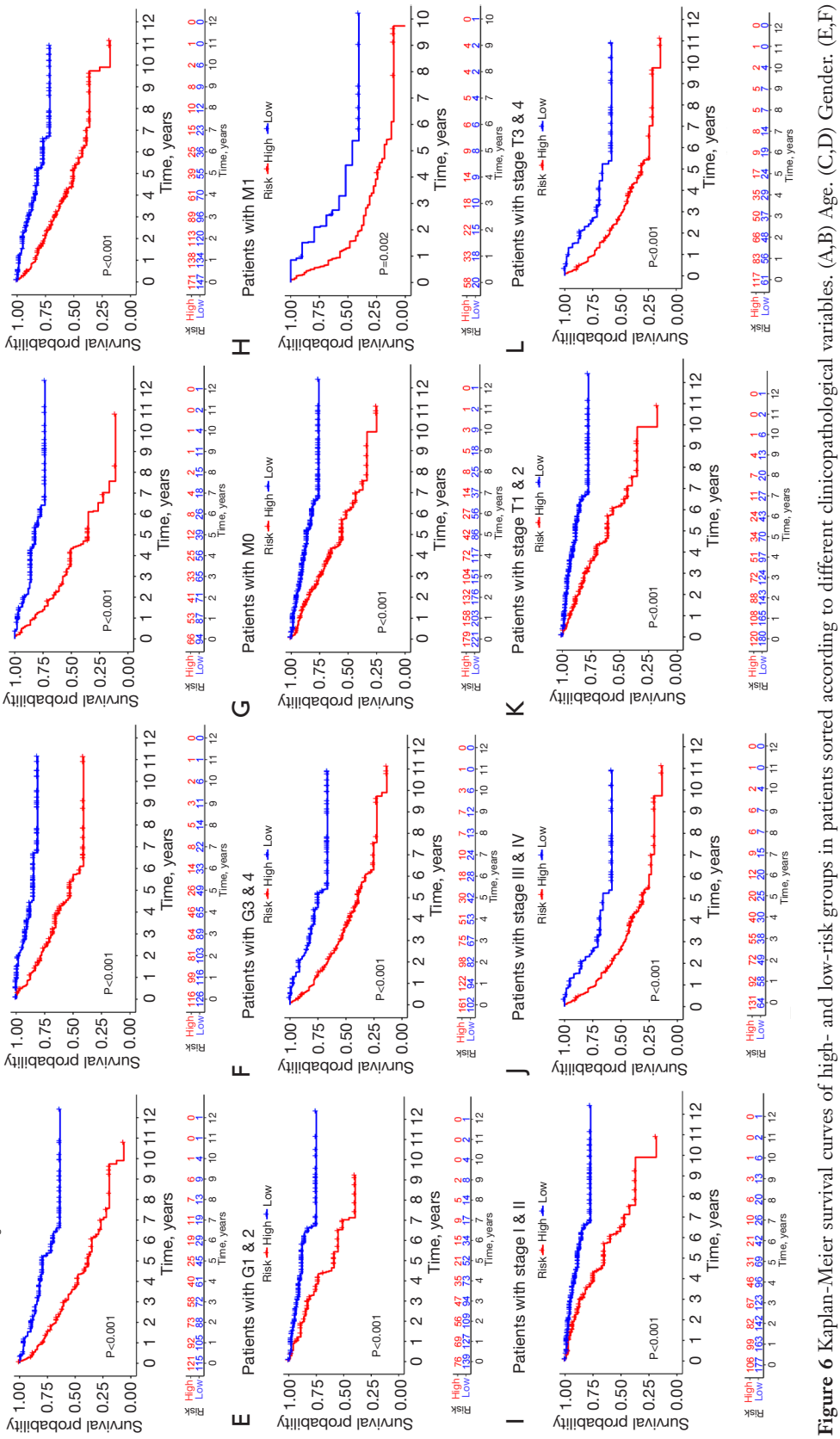

Figure 6 Kaplan-Meier survival curves of high- and low-risk groups in patients sorted according to different clinicopathological variables. (A,B) Age. (C,D) Gender. (E,F) Grade. (G,H) M stage. (I,J) Stage. (K,L) T stage.

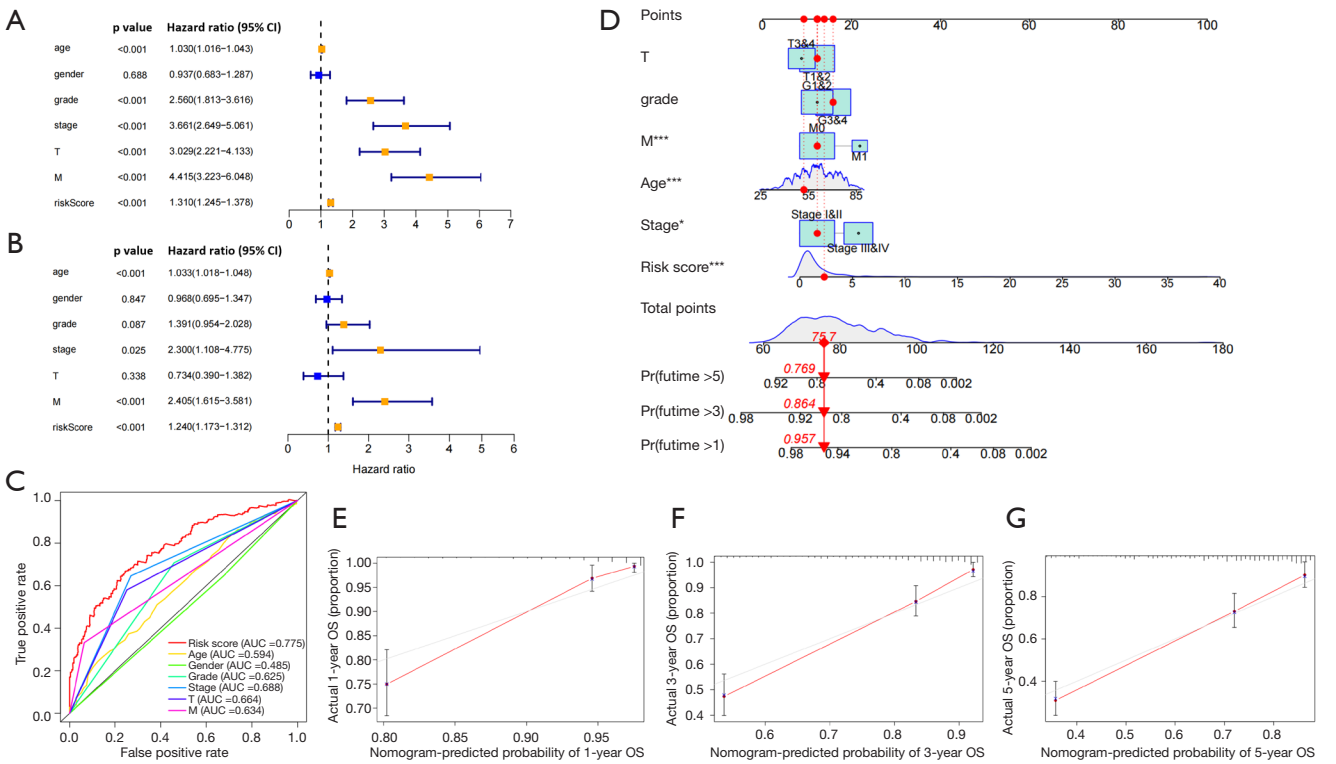

Figure 7 The correlation between the risk score and the prognosis of KIRC patients. (A) Forest plot for univariate Cox regression analysis. (B) Forest plot for multivariate Cox regression analysis. (C) The 5-year time-dependent ROC curve of risk score and clinicopathological variables in the KIRC patients. (D) Nomogram for overall survival at 1-, 2- and 3-year in KIRC patients. (E-G) The calibration curves at 1-, 3- and 5-years for validation to predict the probability of OS. *, P<0.05; ***, P<0.001. CI, confidence interval; KIRC, kidney renal clear cell carcinoma; ROC, time-dependent receiver operating characteristic; AUC, area under the curve; OS, overall survival; T, tumor; M, metastasis.

expressed between the different risk subgroups.

Drug sensitivity analysis

We analyzed the relationship between the risk score and the sensitivity to common anticancer drug agents for KIRC patients (*Figure 10A*). Results demonstrated that patients in the high-risk group possessed lower IC_{50} for bosutinib, camptothecin, paclitaxel, sunitinib, temsirolimus than patients in the low-risk group, indicating that those at high risk are more likely to gain from taking these drugs. On the other hand, the IC_{50} value of bleomycin, sorafenib, pazopanib and lapatinib was higher in the low-risk group. These findings suggested that the risk score could identify patients who are more likely to benefit from appropriate medication.

Analysis of somatic mutations and immune status analysis

To further understand the association between the risk scores and immune status, the enrichment scores of immune cell subpopulations (*Figure 10B*) and their associated functions (*Figure 10C*) were quantified by ssGSEA analysis. The results revealed that $CD8^+$ T cells, macrophages, T helper cells, T follicular helper (Tfh) cells, T helper type 1 (Th1) cells, T helper type 2 (Th2) cells, tumor-infiltrating lymphocyte (TIL) and T regulatory cells (Tregs) tended to be infiltrated more in high-risk group. Conversely, immature dendritic cells (iDCs), mast cells were significantly higher in the low-risk group. Between the two risk groups, Wilcox test confirmed a significant difference in immunological function [including antigen-presenting cell (APC) co-stimulation, cytolytic activity, T cell co-

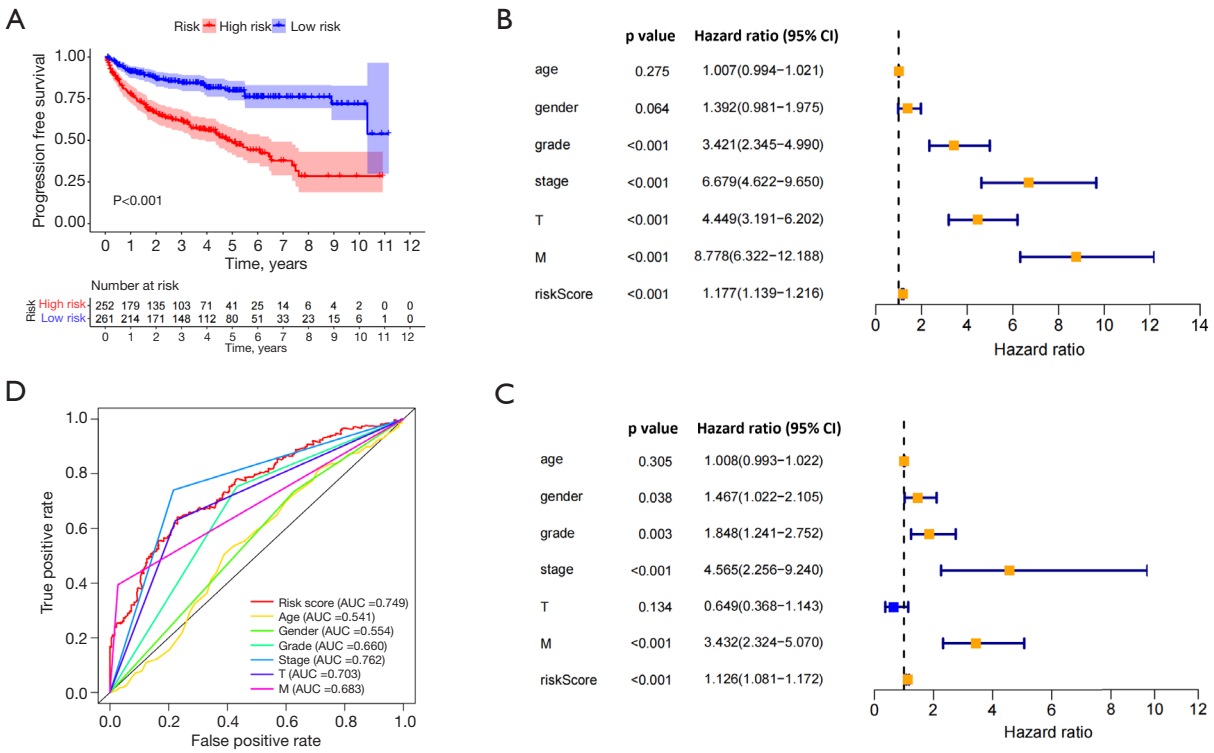

Figure 8 The correlation between the risk score and the PFS of KIRC patients. (A) Survival curves of PFS in KIRC patients. (B) Forest plot for univariate Cox regression analysis. (C) Forest plot for multivariate Cox regression analysis. (D) The 5-year time-dependent ROC curve of risk score and clinicopathological variables in the KIRC patients. CI, confidence interval; PFS, progression-free survival; KIRC, kidney renal clear cell carcinoma; ROC, time-dependent receiver operating characteristic; AUC, area under the curve; T, tumor; M, metastasis.

inhibition, T cell co-stimulation, major histocompatibility complex (MHC) class I, interferon (IFN) response type I/II, and inflammation promoting, etc.]. Subsequently, we evaluated the correlation between the immune checkpoints, including PDCD1, CTLA4, LAG3 and CD27, and risk score, and discovered substantial differences in the two risk groups (*Figure 10D*). These findings indicated that patients may be more prone to respond to immunotherapy in the high-risk group.

Given that the TMB and immunotherapy effectiveness are closely associated, we assessed the value of TMB between the two risk groups. The results revealed a significantly positive correlation between risk score and TMB (*Figure 11A*). As expected, KIRC patients with high TMB tended to have a worse OS (*Figure 11B*). Regardless of whether they were in the low- or high-risk groups, the top three varied genes were *VHL*, *PBRM1*, and *TTN*, as shown in the mutation spectrum in *Figure 11C,11D*.

Discussion

KIRC is the primary subtype of RCC with high heterogeneity and metastatic potential, which originate from renal tubular epithelial cells (23,24). Despite advances in multiple therapeutic methods, more than one hundred thousand KIRC patients die each year because of tumor progression (25). Thus, there is an urgent need to discover novel biomarkers to guide the implementation of individualized treatment and prognosis prediction for KIRC. Recent research has shown that LMR lncRNAs are important for understanding the prognosis of several cancer patients. However, the research on the function of LMR lncRNAs in KIRC is blank.

Here, we established a LMR lncRNA signature to accurately predict the prognosis of KIRC patients and provide an important reference for individualized treatment. Firstly, we selected six prognostic-associated

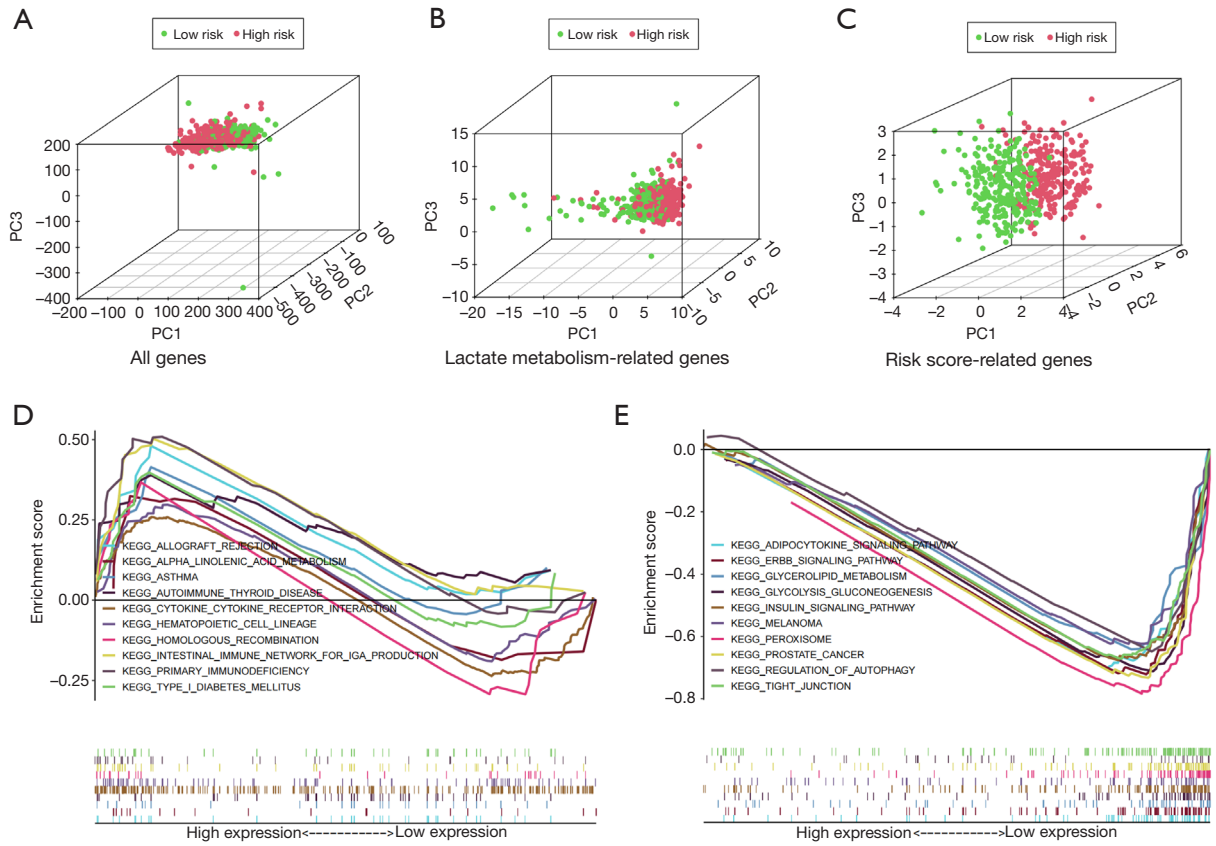

Figure 9 Principal component analyses and functional enrichment analysis. (A-C) Results of principal component analyses for all genes, lactate metabolism-related genes, and risk score-related genes in TCGA entire set. (D) Gene Set Enrichment Analysis for the high-risk groups. (E) Gene Set Enrichment Analysis for the low-risk groups. TCGA, The Cancer Genome Atlas; PC, principal component.

LMR lncRNAs that were differentially expressed in normal and KIRC tissues, and constructed a prognostic signature by using multivariate regression Cox regression analysis. After classifying KIRC patients into two risk groups, we performed survival analyses to assess their predictive power. The results confirmed that the OS and PFS of patients in the high-risk group was significantly shortened than low-risk group. Moreover, stratified analysis indicated that the LMR lncRNA signature retained a high level in predicting the prognosis in various indicators (including age, gender, grade, AJCC stages, T stage and M stage). In the present study, we also found that this signature can serve as a predictor of the responsiveness to anticancer drug agents, including immune checkpoint inhibitors, in KIRC. Collectively, we generated a LMR lncRNAs prognostic signature that could be served as an independent biomarker of KIRC.

One of these six signature-related lncRNAs, *LINC00944*, was first reported by Chen *et al.* (26) and was found to be elevated in RCC tissues and cell lines, and significantly correlated with tumor stage and prognosis in RCC (26,27). Additionally, *LINC00944* was linked to immune microenvironment, ferroptosis, and oxidative stress, and it may be used to predict the prognosis of several cancers, including KIRC (26-30). lncRNA *AL162377.1*, which supported *SYDE2* expression downregulation and was associated with tumor immune infiltration, was another important lncRNA for predicting the outcomes of KIRC patients (31). Previous studies have reported that *AP001267.3*, which is related to immune, could serve as key lncRNAs to construct prognostic signatures for patients with papillary RCC (32). Although the significance of the lncRNA *AC090772.3* in the advancement of hepatocellular carcinoma has been proposed (33), its function in kidney cancer is yet to be understood. However, the role of the remaining two LMR lncRNAs (*Z83745.1*, *AC092296.1*) in

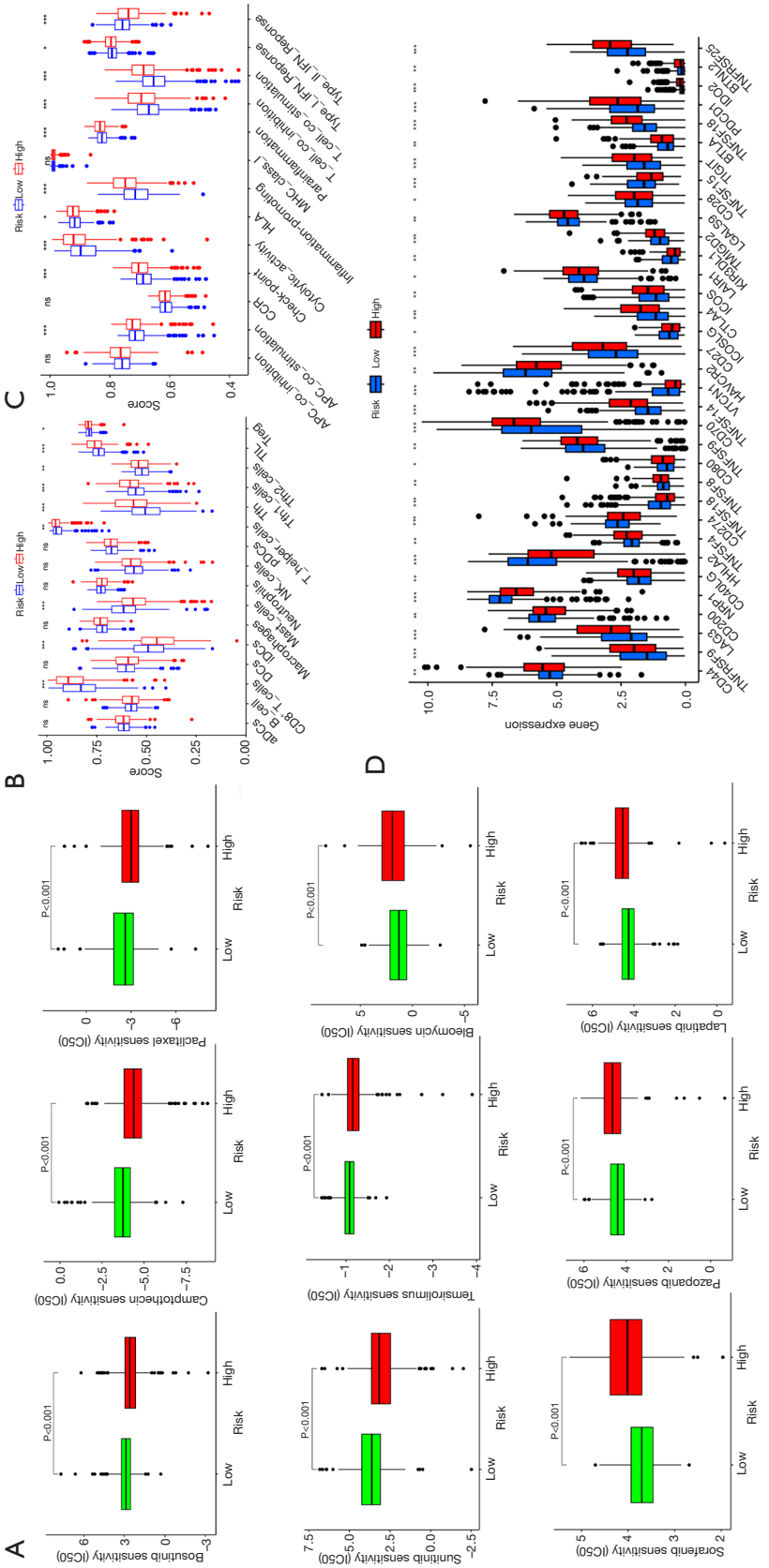

Figure 10 Estimation of the associations between drugs sensitivity, immune infiltration level and the risk score. (A) IC50 of various drugs in high-risk and low-risk groups. (B) ssGSEA algorithm was used to calculate the infiltration levels of immune cells in high- and low-risk groups. (C) Correlation between the risk score and immune-related functions. (D) Expression of immune checkpoints among high- and low-risk groups. * , P<0.05; ** , P<0.01; *** , P<0.001; ns, non-significant. ssGSEA, single sample gene set enrichment analysis; aDCs, activated dendritic cells; iDCs, immature dendritic cells; NK, natural killer; pDCs, plasmacytoid dendritic cells; Tfh, T follicular helper; Th1, T helper type 1; Th2, T helper type 2; TIL, tumor-infiltrating lymphocyte; Treg, T regulatory cell; APC, antigen-presenting cell; CCR, chemokine receptor; HLA, human leukocyte antigen; MHC, major histocompatibility complex; IFN, interferon.

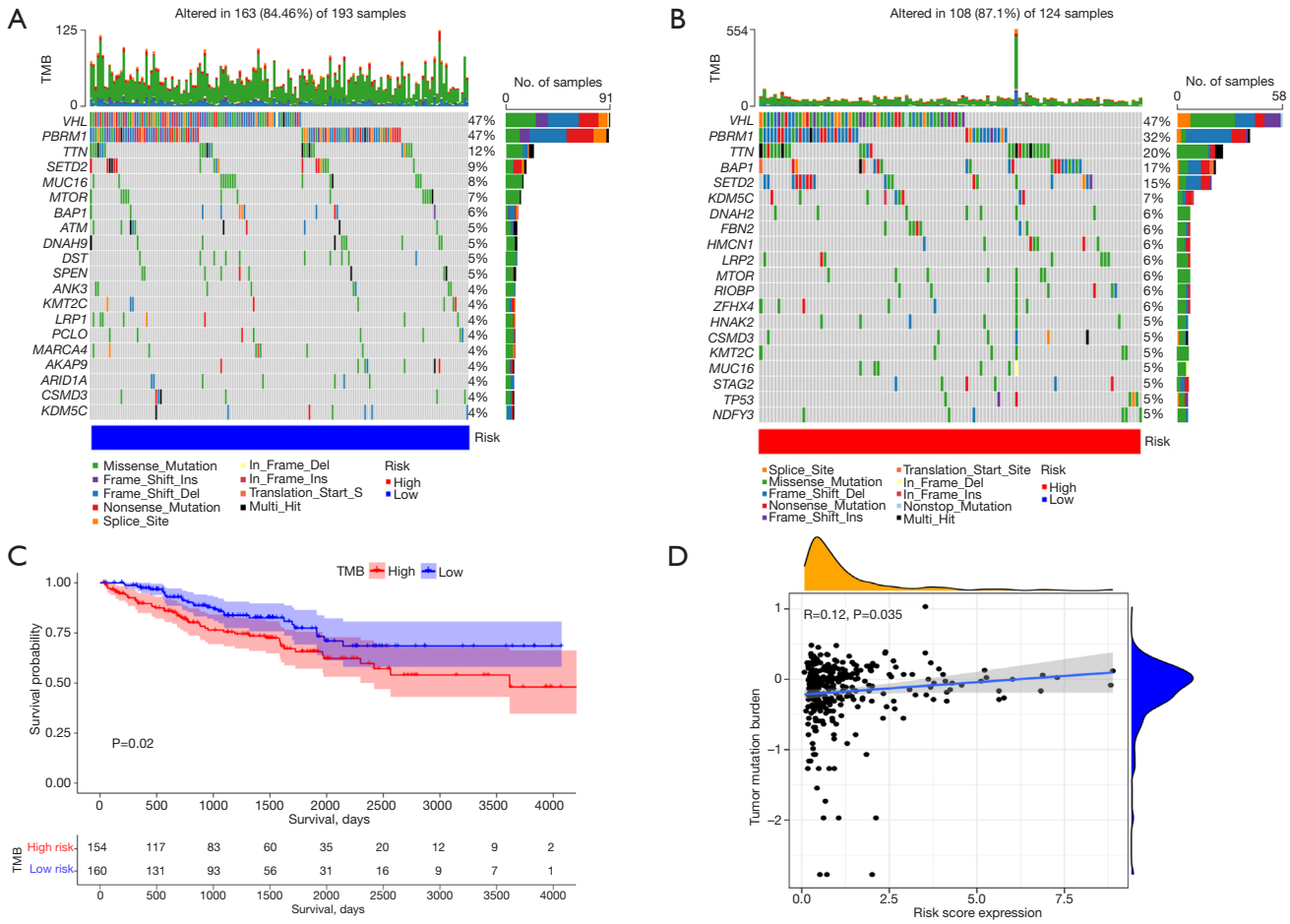

Figure 11 Tumor somatic mutational analyses between high- and low-risk groups. (A,B) Mutation spectrum of the top 20 mutated genes in the high- and low-risk groups. (C) Survival analysis of the TMB-defined groups. (D) The relevance of tumor mutational burden with the risk score was revealed through the correlation analysis. TMB, tumor mutational burden.

other diseases or malignancies has not yet been reported. Therefore, it is urgent to verify the role of these LMR lncRNAs in KIRC patients.

KIRC characterized by a pronounced reliance on aerobic glycolysis, fundamentally presents as a metabolic disease distinguished by a reprogramming of energy metabolism (7,34). Enhanced glycolysis in tumor cells leads to elevated lactate levels, contributing to tumor microenvironment (TME) acidification. TME consists of tumor cells, various immune and non-immune cells (13). Remarkably, the acidic milieu in the TME can foster immune suppression, inhibit cytotoxic T cell activity, and promote the recruitment of immunosuppressive cell populations such as regulatory T cells and M2-like macrophages. Additionally, the acidic conditions may impair APC function and diminish the efficacy of cytotoxic T cells (7). In the present study, we found that patients in the high-risk group had a higher proportion of $CD8^+$ T cells, macrophages, T helper cells, Tfh cells, Th1 cells, Th2 cells, TILs, and regulatory T cell compared to those in the low-risk group. The GSEA results revealed a predominant presence of immune-related pathways in high-risk KIRC patients, providing valuable insights into their potential significance in TME. Earlier research has demonstrated that the acidic pH in the TME also impacts the efficacy of immunotherapeutic agents (7). In the present study, significant differences were excited in the expression of immune checkpoints between the two risk groups, which were linked to the immunosuppressive microenvironment (35). We also observed that the risk score was positively correlated with the TMB. Moreover, accumulating evidence suggests that a subpopulation of cells within tumors, known as cancer stem cells (CSCs), possesses

unique characteristics that contribute to tumor recurrence, metastasis, and resistance to conventional treatments. Lactic acid may play a role in metabolic adaptations of CSCs, influencing their preference for glycolytic or oxidative phosphorylation pathways based on contextual factors like oxygen tension and glucose availability (36). These findings suggested that the LMR lncRNAs may contribute to the discovery of regulatory mechanisms of tumor immunity and tumor progression.

There are some limitations to this study. Firstly, we did not apply the data from other databases for external validation to test the applicability of the prognostic signature. Secondly, the lack of *in-vivo* and *in-vitro* experiments would lead to insufficient evidence for this model.

Conclusions

We developed a novel prognostic signature based on seven LMR lncRNA for KIRC patients and verified its stable prognostic predictive utility. The signature was also correlated with the level of immune infiltration, TMB scores, and drug sensitivity. In conclusion, our study revealed that the LMR lncRNA predictive signature has prospective clinical implications for prognosis evaluation and might guide clinicians in making rational treatment decisions.

Acknowledgments

Funding: None.

Footnote

Reporting Checklist: The authors have completed the TRIPOD reporting checklist. Available at https://tau.amegroups.com/article/view/10.21037/tau-23-483/rc

Data Sharing Statement: Available at https://tau.amegroups.com/article/view/10.21037/tau-23-483/dss

Peer Review File: Available at https://tau.amegroups.com/article/view/10.21037/tau-23-483/prf

Conflicts of Interest: All authors have completed the ICMJE uniform disclosure form (available at https://tau.amegroups.com/article/view/10.21037/tau-23-483/coif). The authors have no conflicts of interest to declare.

Ethical Statement: The authors are accountable for all aspects of the work in ensuring that questions related to the accuracy or integrity of any part of the work are appropriately investigated and resolved. The study was conducted in accordance with the Declaration of Helsinki (as revised in 2013).

References

1. Miller KD, Nogueira L, Mariotto AB, et al. Cancer treatment and survivorship statistics, 2019. CA Cancer J Clin 2019;69:363-85.
2. Siegel RL, Miller KD, Fuchs HE, et al. Cancer Statistics, 2021. CA Cancer J Clin 2021;71:7-33.
3. Padala SA, Barsouk A, Thandra KC, et al. Epidemiology of Renal Cell Carcinoma. World J Oncol 2020;11:79-87.
4. Mendoza-Alvarez A, Guillen-Guio B, Baez-Ortega A, et al. Whole-Exome Sequencing Identifies Somatic Mutations Associated With Mortality in Metastatic Clear Cell Kidney Carcinoma. Front Genet 2019;10:439.
5. Gao J, Yang D, Xu H, et al. ADAM metallopeptidase domain 12 overexpression correlates with prognosis and immune cell infiltration in clear cell renal cell carcinoma. Bioengineered 2022;13:2412-29.
6. Escudier B, Porta C, Schmidinger M, et al. Renal cell carcinoma: ESMO Clinical Practice Guidelines for diagnosis, treatment and follow-up†. Ann Oncol 2019;30:706-20.
7. Lasorsa F, Rutigliano M, Milella M, et al. Cellular and Molecular Players in the Tumor Microenvironment of Renal Cell Carcinoma. J Clin Med 2023;12:3888.
8. Kennedy LB, Salama AKS. A review of cancer immunotherapy toxicity. CA Cancer J Clin 2020;70:86-104.
9. Braun DA, Street K, Burke KP, et al. Progressive immune dysfunction with advancing disease stage in renal cell carcinoma. Cancer Cell 2021;39:632-648.e8.
10. Abdel-Wahab AF, Mahmoud W, Al-Harizy RM. Targeting glucose metabolism to suppress cancer progression: prospective of anti-glycolytic cancer therapy. Pharmacol Res 2019;150:104511.

11. Lv X, Lv Y, Dai X. Lactate, histone lactylation and cancer hallmarks. Expert Rev Mol Med 2023;25:e7.
12. Li X, Yang Y, Zhang B, et al. Lactate metabolism in human health and disease. Signal Transduct Target Ther 2022;7:305.
13. Sun Z, Tao W, Guo X, et al. Construction of a Lactate-Related Prognostic Signature for Predicting Prognosis, Tumor Microenvironment, and Immune Response in Kidney Renal Clear Cell Carcinoma. Front Immunol 2022;13:818984.
14. Certo M, Tsai CH, Pucino V, et al. Lactate modulation of immune responses in inflammatory versus tumour microenvironments. Nat Rev Immunol 2021;21:151-61.
15. Ying M, You D, Zhu X, et al. Lactate and glutamine support NADPH generation in cancer cells under glucose deprived conditions. Redox Biol 2021;46:102065.
16. Panni S, Lovering RC, Porras P, et al. Non-coding RNA regulatory networks. Biochim Biophys Acta Gene Regul Mech 2020;1863:194417.
17. Tan YT, Lin JF, Li T, et al. LncRNA-mediated posttranslational modifications and reprogramming of energy metabolism in cancer. Cancer Commun (Lond) 2021;41:109-20.
18. Simion V, Haemmig S, Feinberg MW. LncRNAs in vascular biology and disease. Vascul Pharmacol 2019;114:145-56.
19. Tsai KW, Lo YH, Liu H, et al. Linc00659, a long noncoding RNA, acts as novel oncogene in regulating cancer cell growth in colorectal cancer. Mol Cancer 2018;17:72.
20. Xiao J, Wang X, Liu Y, et al. Lactate Metabolism-Associated lncRNA Pairs: A Prognostic Signature to Reveal the Immunological Landscape and Mediate Therapeutic Response in Patients With Colon Adenocarcinoma. Front Immunol 2022;13:881359.
21. Jiang T, Zhou W, Chang Z, et al. ImmReg: the regulon atlas of immune-related pathways across cancer types. Nucleic Acids Res 2021;49:12106-18.
22. Livak KJ, Schmittgen TD. Analysis of relative gene expression data using real-time quantitative PCR and the 2(-Delta Delta C(T)) Method. Methods 2001;25:402-8.
23. Ravindranathan D, Alhalabi O, Rafei H, et al. Landscape of Immunotherapy in Genitourinary Malignancies. Adv Exp Med Biol 2021;1342:143-92.
24. Hsieh JJ, Purdue MP, Signoretti S, et al. Renal cell carcinoma. Nat Rev Dis Primers 2017;3:17009.
25. Capitanio U, Montorsi F. Renal cancer. Lancet 2016;387:894-906.
26. Chen C, Zheng H. LncRNA LINC00944 Promotes Tumorigenesis but Suppresses Akt Phosphorylation in Renal Cell Carcinoma. Front Mol Biosci 2021;8:697962.
27. Zhang Y, Zhou G, Shi W, et al. A novel oxidative-stress related lncRNA signature predicts the prognosis of clear cell renal cell carcinoma. Sci Rep 2023;13:5740.
28. de Santiago PR, Blanco A, Morales F, et al. Immune-related IncRNA LINC00944 responds to variations in ADAR1 levels and it is associated with breast cancer prognosis. Life Sci 2021;268:118956.
29. Zhou Z, Yang Z, Cui Y, et al. Identification and Validation of a Ferroptosis-Related Long Non-Coding RNA (FRlncRNA) Signature to Predict Survival Outcomes and the Immune Microenvironment in Patients With Clear Cell Renal Cell Carcinoma. Front Genet 2022;13:787884.
30. Xue Q, Wang Y, Zheng Q, et al. Construction of a prognostic immune-related lncRNA model and identification of the immune microenvironment in middle- or advanced-stage lung squamous carcinoma patients. Heliyon 2022;8:e09521.
31. Shen C, Chen Z, Jiang J, et al. A new CCCH-type zinc finger-related lncRNA signature predicts the prognosis of clear cell renal cell carcinoma patients. Front Genet 2022;13:1034567.
32. Liu Y, Gou X, Wei Z, et al. Bioinformatics profiling integrating a four immune-related long non-coding RNAs signature as a prognostic model for papillary renal cell carcinoma. Aging (Albany NY) 2020;12:15359-73.
33. Tang Y, Zhang H, Chen L, et al. Identification of Hypoxia-Related Prognostic Signature and Competing Endogenous RNA Regulatory Axes in Hepatocellular Carcinoma. Int J Mol Sci 2022;23:13590.
34. Vuong L, Kotecha RR, Voss MH, et al. Tumor Microenvironment Dynamics in Clear-Cell Renal Cell Carcinoma. Cancer Discov 2019;9:1349-57.
35. Xin S, Mao J, Cui K, et al. A cuproptosis-related lncRNA signature identified prognosis and tumour immune microenvironment in kidney renal clear cell carcinoma. Front Mol Biosci 2022;9:974722.
36. Lasorsa F, Rutigliano M, Milella M, et al. Cancer Stem Cells in Renal Cell Carcinoma: Origins and Biomarkers. Int J Mol Sci 2023;24:13179.

Cite this article as: Xu T, Liu Y, Ning B, Luo M, Wei Y. Identification of a lactate metabolism-related lncRNAs signature for predicting the prognosis in patients with kidney renal clear cell carcinoma. Transl Androl Urol 2024;13(4):509-525. doi: 10.21037/tau-23-483

Supplementary

Table S1 The primer sequences of genes

Gene	Pimier Sequences of Genes	
	Forward primier (5'-3')	Reverse primier (3'-5')
GAPDH	GGAGTCCACTGGCGTCTTCA	GTCATGAGTCCTTCCACGATACC
LINC00944	CTCTTAATCCTCTGTCCTCCATCA	AGTCATTCCATTCCACAGTCTCT
AC092296.1	CCCGCTGCCTTCCTAAAGAA	AGTAGACGGAGGGAGCAAGT

https://dx.doi.org/10.21037/tau-23-483